

RESEARCH ARTICLE

The influence on oxidative stress markers, inflammatory factors and intestinal injury-related molecules in Wahui pigeon induced by lipopolysaccharide

Fei Wang¹, Jin Liu¹, Xiaofen Hu¹, Youbao Zhong², Feng Wen³, Xiaoen Tang⁴, Shanshan Yang¹, Shengwei Zhong¹, Zuohong Zhou¹, Xu Yuan¹, Yong Li^{1*}

1 College of Animal Science and Technology, Jiangxi Agricultural University, Nanchang, 330045, Jiangxi, China, **2** Technology Center of Experimental Animals, Jiangxi University of Traditional Chinese Medicine, Nanchang, 330004, Jiangxi, China, **3** College of Life Science and Engineering, Foshan University, Foshan, 528231, Guangdong, China, **4** Fuzhou Husbandry Breeding Farm, Linchuan, 344000, Jiangxi, China

* liyong2912@163.com



OPEN ACCESS

Citation: Wang F, Liu J, Hu X, Zhong Y, Wen F, Tang X, et al. (2021) The influence on oxidative stress markers, inflammatory factors and intestinal injury-related molecules in Wahui pigeon induced by lipopolysaccharide. *PLoS ONE* 16(5): e0251462. <https://doi.org/10.1371/journal.pone.0251462>

Editor: Rosanna Di Paola, University of Messina, ITALY

Received: December 13, 2020

Accepted: April 27, 2021

Published: May 12, 2021

Copyright: © 2021 Wang et al. This is an open access article distributed under the terms of the [Creative Commons Attribution License](https://creativecommons.org/licenses/by/4.0/), which permits unrestricted use, distribution, and reproduction in any medium, provided the original author and source are credited.

Data Availability Statement: All relevant data are within the paper and its [Supporting Information](#) files.

Funding: This work was supported by grants from the National Natural Science Foundation Project of China (No. 31960688 and 31360592) and the Natural Science Foundation Project of Jiangxi Province (No. 20181BAB204016). The funders and Fuzhou Husbandry Breeding Farm had no role in study design, data collection and analysis, decision to publish, or preparation of the manuscript. There

Abstract

Introduction

The intestinal structure is the foundation for various activities and functions in poultry. An important question concerns the changes in the intestinal status under endotoxin stimulation. This study aimed to investigate the mechanism of intestinal injury induced by lipopolysaccharide (LPS) in Wahui pigeons.

Methods

Thirty-six 28-day-old healthy Wahui pigeons were randomly divided into two groups. The experimental group was injected with LPS (100 µg/kg) once per day for five days, and the control group was treated with the same amount of sterile saline. Blood and the ileum were collected from pigeons on the first, third, and fifth days of the experiment and used for oxidative stress assessment, inflammatory factor detection, histopathological examination, and positive cell localization. In addition, intestinal injury indices and mRNA expression levels (tight junction proteins, inflammatory cytokines, and factors related to autophagy and apoptosis) were evaluated.

Results

Villi in the ileum were shorter in the LPS group than in the control group, and D-lactic acid levels in the serum were significantly increased. Glutathione and catalase levels significantly decreased, but the malondialdehyde content in the serum increased. TNF-α and IL-10 were detected at higher levels in the serum, with stronger positive signals and higher mRNA expression levels, in the LPS group than in the control group. In addition, the levels of TLR4, MyD88, NF-κB, and HMGB1 in the inflammatory signaling pathway were also upregulated.

was no other additional funding received for this study.

Competing interests: The authors have declared that no competing interests exist. This commercial affiliation does not alter our adherence to PLOS ONE policies on sharing data and materials.

Finally, the mRNA expression of Claudin3, Occludin, and ZO-1 was significantly decreased; however, that of Beclin1 and Atg5 was increased in the LPS group.

Conclusion

Ileal pathological changes and oxidative stress were caused by LPS challenge; it is proposed that this triggering regulates the inflammatory response, causing excessive autophagy and apoptosis, promoting intestinal permeability, and leading to intestinal injury in Wahui pigeons.

1. Introduction

It is well known that poultry meat is very popular owing to its competitive price, lack of religious and geographical restrictions, and high nutritional value [1]. Pigeon meat contains a high protein and low fat content, and its digestion and absorption rate can reach more than 91%. However, in pigeons bred for meat, salmonellosis frequently occurs. This disease can lead to fever, dysentery, arthritis, neurological symptoms, or acute septicemia in later stages, with high mortality in squabs. LPS, which is a known endotoxin, is a key molecule in the outer membrane of gram-negative bacteria, and is considered a main pathogenic factor [2]. During endotoxemic shock, immune cells release several mediators and cytokines that lead to hypotension, fever and tissue injury [3]. Stimulation with LPS has extensively been employed in many endotoxic models for the understanding of underlying complex molecular mechanisms of endotoxin-mediated acute intestine tissue damage [4–7].

LPS can cause oxidative stress by promoting the formation of reactive oxygen species (ROS) in several cell types [4,8], indicating that oxidative stress plays an important role in the pathogenesis of LPS. Oxidative stress induced by ROS is closely related to inflammatory responses [9]. High LPS exposure can increase the production of ROS and take a regulatory role in inflammation, leading to peripheral inflammation in many models [10]. Excessive ROS can cause oxidative stress, autophagy, and apoptosis in hepatocytes [11,12]. In addition, LPS can promote epithelial cell apoptosis and proliferation and induce proinflammatory processes that cause inflammatory responses through the nuclear factor- κ B (NF- κ B) signaling pathway [13].

Inflammation is a protective reaction to infections and tissue damage that is triggered by innate immunocytes responding to external stimuli [14]. Immune cells can initiate signaling cascades that activate crucial transcription factors, including NF- κ B, mitogen-activated protein kinases (MAPKs), and activator protein 1, which in turn regulate inflammation-specific genes [15,16]. The interaction between LPS and Toll-like receptor 4 (TLR4) leads to the formation of an LPS signaling complex consisting of surface molecules, including myeloid differentiation primary response gene 88 (MyD88), toll-interleukin-1 receptor domain-containing adapter inducing interferon β , and TNF- α receptor association factor 6, and the activation of transcription factors, which then induce the activation of the inflammatory response [17].

The intestinal barrier is considered to be a selective barrier against exogenous noxious antigens and pathogens [18]. Disruption of the intestinal barrier promotes the transit of luminal antigens to the subepithelial tissues, inducing mucosal and systemic inflammatory responses, which is the major pathogenesis in intestinal disease [19]. Multiple factors, including inflammation and oxidative stress, can cause intestinal barrier damage [18–21]. Evidence has demonstrated that LPS stimulates intestinal immune cells to rapidly produce proinflammatory cytokines, which leads to structural and functional injury in the intestine [22]. Furthermore, exposure to

intraperitoneal LPS at low doses to laboratory animals can selectively increase intestinal permeability by tight junction modulation and cause a pro-inflammatory state in the intestine [23]. The mucosal immune system is well known as an important part of the entire immune network in poultry. As an independent immune system, it plays critical roles with unique structure-function features in fighting against infections [24]. Intestinal mucosa is not only the crucial site for food digestion and nutrient absorption but also an immune structure, where the largest number of immune cells collectively presents to form a strict defense system [25]. Therefore, normal intestinal structure plays a key role for its immunity. The current study explored the dynamic changes in the intestinal microstructure, degree of oxidative stress, expression of inflammatory factors, and activity of autophagy, apoptosis in Wahui pigeons induced by *Salmonella* LPS. The objective was to clarify the pathogenic mechanism of intestinal injury in pigeons with LPS treatment and to provide theoretical evidence for intestinal immunity.

2. Materials and methods

Experimental animals

In this experiment, thirty-six 28-day-old healthy Wahui pigeons (body weight: 0.47 ± 0.05 kg) were purchased from Pigeon Farm (Nanchang, Jiangxi, China) and had *ad libitum* access to feed and water. After two days of pre-feeding to alleviate any stress response, the pigeons were randomly divided into two groups. The LPS group was injected intraperitoneally with LPS (L6511; Sigma-Aldrich, St. Louis, MO, USA) at $100 \mu\text{g}/\text{kg}$ body weight every day, and the control group was injected with the same volume of saline. On the first, third, and fifth days of the experiment, six pigeons were randomly selected from each group for blood collection (5 mL) after a *anaesthetization* by CO₂ inhalation. Subsequently, we dissected the abdominal cavity and instantly harvested the ileum samples. Parts of the ileum was fixed in Bouin's solution and 4% paraformaldehyde for 24–72 h, and the remaining portion was quickly placed in liquid nitrogen and then stored in a freezer at -80°C . All procedures in this experiment were approved by the Institutional Animal Care and Use Committee of Jiangxi Agricultural University (approval number: JXAULL-2020-35).

Detection of biochemical and antioxidant indices in the serum

The main compounds of interest in the serum were superoxide dismutase (SOD), catalase (CAT), glutathione (GSH), and malondialdehyde (MDA), which were evaluated by using a spectrophotometric method according to the corresponding diagnostic kits (Nanjing Jiancheng Bioengineering Institute Inc., Nanjing, Jiangsu, China). The content of D-lactic acid (D-LA) in the serum was measured using enzyme-linked immunosorbent assay (ELISA). The method was carried out according to the instructions for the serum ELISA kit (Nanjing Jiancheng Bioengineering Institute Inc.).

Detection of inflammatory factors in the serum

HMGB1, TNF- α , and IL-10 concentrations in the serum were measured by ELISA according to the corresponding kit instructions (Nanjing Jiancheng Bioengineering Institute Inc.). The concentrations of HMGB1, TNF- α , and IL-10 were calculated according to a standard curve and are expressed as ng/L.

Hematoxylin-eosin (HE) staining

Fixed tissues were rinsed with running water for 5–10 h and then dehydrated in 70%, 80%, 90%, 95%, and anhydrous ethanol using a LEICA ASP200S automatic dehydrator (LEICA

Camera AG, Wetzlar, Germany). Samples were then rinsed in xylene three times and dipped in paraffin for 3–4 h. Then, 4- μ m-thick sections were made with a LEICA semiautomatic microtome (LEICA Camera AG). Half of the sections were processed by HE staining, and the other half was used for immunohistochemical staining, as previously described [26]. The tissue sections were sequentially subjected to two rinses in xylene and two rinses in anhydrous ethanol, 95%, 90%, 80%, and 70% ethanol and then stained in a 1% hematoxylin solution for 1 min. Subsequently, the sections were rapidly processed through a color separation solution and blue-black fluid and dyed in an eosin solution for 30–45 s. Finally, the sections were dehydrated in 70%, 80%, 90%, 95%, and anhydrous ethanol; rinsed twice in xylene; and then mounted with neutral balsam and cover slips. The intestinal microstructure was observed and imaged using an Olympus BX53 microscope (Olympus, Japan), and ten villus heights (VH) and ten crypt depths (CD) were measured in each visual field. Ten visual fields were evaluated in each section at random, and the ratio of villus height/crypt depth (VH/CD) was calculated.

Immunohistochemical staining

Immunohistochemistry was performed as previously described [27]. After deparaffinization, an endogenous peroxidase blocking solution was added to tissue sections, which were then incubated at 37°C for 15 min. Antigen retrieval was performed at 98°C for 12 min, and then the sections were incubated with goat serum at 37°C for 20 min. Rabbit anti-TNF- α (1:600) and mouse anti-IL-10 (1:250) polyclonal antibodies were added dropwise to the sections and incubated at 4°C overnight. After the primary antibody was ligated, the sections were incubated with biotinylated goat anti-rabbit and goat anti-mouse secondary antibodies at 37°C for 30 min, combined with peroxidase-labeled streptavidin at room temperature for 10 min, and then visualized using a DAB coloring agent for 1–5 min. The sections were counterstained in a hematoxylin solution for 2 min, processed in 1 mL/L hydrochloric acid alcohol differentiation and blue-black fluid, and rinsed with distilled water. Finally, the sections were dehydrated, cleared and mounted with neutral balsam and cover slips. The primary antibody was replaced with a 0.01 mol/L PBS solution in the control group, but the remaining steps were performed as described above. All sections were observed and imaged using an Olympus BX53 microscope (Olympus, Japan), and six fields of vision were chosen according to different regions of each ileum section. Image-Pro Plus (IPP) 6.0 software (Media Cybernetics, USA) was used to calculate the integral optical density (IOD) for positive staining and the graphs were prepared by Prism software version 8.0 (GraphPad Software, Inc., San Diego, USA). The average optical density (AOD = IOD/area) was calculated.

RNA extraction and cDNA synthesis

RNA was extracted from the ileum using a TRIzol extraction method. Briefly, frozen specimens were powdered in liquid nitrogen and homogenized in RNAiso Plus (TAKARA Bio Inc., Shiga, Japan); then, 500 μ L of sample was transferred to a tube. Chloroform (200 μ L) was added to each tube, and the tubes were violently shaken for 15 s and centrifuged at 4°C and 12000 rpm for 15 min. Each sample was divided into three layers: the yellow organic phase, middle layer, and upper colorless water phase. The upper water phase was transferred to a new 1.5-mL tube, and then 500 μ L of isopropanol was added to this tube and mixed gently. The mixture was kept at room temperature for 10 min and then centrifuged at 4°C and 12000 rpm for 10 min. After the supernatant was discarded, the isolated total RNA was washed with 1 mL of 95% ethanol prepared with RNase-free double-distilled water. Then, 30 μ L of diethylpyrocarbonate water (TAKARA Bio Inc.) was added to fully dissolve the precipitate, which was then placed in a freezer at -80°C (Thermo Fisher Scientific, Waltham, MA, USA). RNA

concentration and optical density values were detected using an ultraviolet spectrophotometer (Beckman Coulter Inc., Brea, CA, USA). First-strand cDNA was synthesized using the Easy-Script One-Step gDNA Removal and cDNA Synthesis SuperMix Kit (TransGen Biotech Co., Ltd., Beijing, China) and then placed in a freezer at -20°C .

Quantitative real-time PCR detection

The mRNA expression of related genes in the ileum was detected by real-time fluorescence quantitative PCR. The cDNA generated from each tissue sample was used as a template, and the *GAPDH* gene was used as an internal reference. The reaction system had a total volume of 20 μL and consisted of the following components: 10 μL of $2 \times$ qPCR Mix, 0.4 μL of 10 $\mu\text{mol/L}$ upstream and downstream primers (S1 Table), 2 μL of cDNA, and 7.2 μL of nuclease-free water. The PCR conditions were as follows: predenaturation of the template at 94°C for 30 s and a total of 42 cycles of 94°C for 5 s and 62°C for 30 s for template amplification, with a final slow increase in temperature by 0.5°C every 10 s from 55°C to 95°C . Results were calculated using the $2^{-\Delta\Delta\text{Ct}}$ method.

Statistical analysis

One-way analysis of variance was performed to compare differences between the control and LPS groups using SPSS 17.0 software (Chicago, IL, USA), and differences were considered significant if $p < 0.05$ (* $p < 0.05$, ** $p < 0.01$). All data are presented as the mean \pm standard deviation. Graph Prism 8.0 software (GraphPad, San Diego, CA, USA) was used to generate the corresponding graphs.

3. Results

Effects of LPS on antioxidant indices

Oxidative stress is a critical factor involved in the barrier disruption in intestinal diseases [28]. It can destroy essential cellular molecules, such as lipids, proteins, and DNA, resulting in a series of diseases, including intestinal barrier injury [20]. Therefore, several antioxidant indices were tested for evaluating oxidative stress. Compared with those in the control group, the activity of catalase (CAT) and content of glutathione (GSH) in the LPS group were significantly decreased in the serum on the first, third, and fifth days, while the malondialdehyde (MDA) content was increased on the first and third days (Fig 1A, 1B and 1D). Superoxide dismutase (SOD) showed lower activity in the serum of LPS-treated Wuhui pigeons than in that of saline-treated Wuhui pigeons (Fig 1C).

Effects of LPS on inflammatory factors

According to enzyme-linked immunosorbent assay (ELISA) results (Fig 2), the concentrations of TNF- α and IL-10 were significantly greater in LPS-treated pigeons than in saline-treated pigeons on day 1 ($p < 0.01$), while the concentration of HMGB1 showed no significant difference between the two groups ($p > 0.05$). The TNF- α , HMGB1, and IL-10 concentrations were extremely significantly greater in LPS-treated Wuhui pigeons than in saline-treated pigeons on days 3 and 5 ($p < 0.01$).

Effects of LPS on intestinal function and morphology

D-LA is a chemical marker that is usually present at low levels in the circulatory system of healthy individuals; these levels increase significantly with the destruction of the intestinal barrier [29]. After LPS stimulation, on the first, third, and fifth days, D-LA levels were

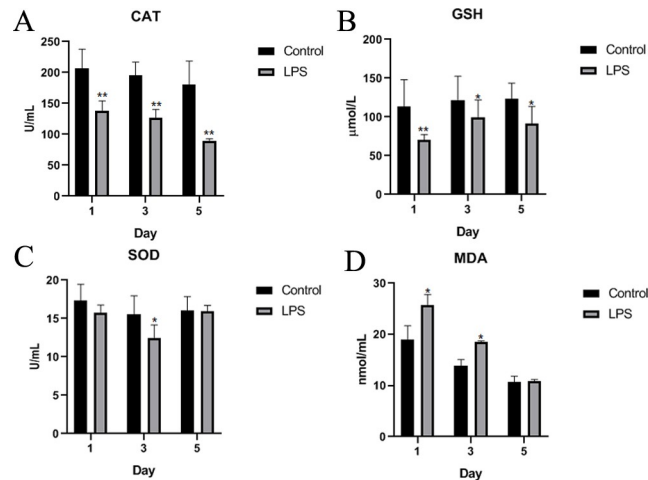


Fig 1. Antioxidant indices of Wahui pigeons treated with LPS or saline. The antioxidant indices of Wahui pigeons were detected in both groups on the first, third, and fifth days. Data represent the mean \pm standard deviation ($n = 6$ in each group); * $p < 0.05$, ** $p < 0.01$. Abbreviations: CAT—catalase; GSH—glutathione; SOD—superoxide dismutase; MDA—malondialdehyde.

<https://doi.org/10.1371/journal.pone.0251462.g001>

significantly higher in the LPS-treated pigeons than in the saline-treated pigeons evaluated on the same date ($p < 0.01$ for all three days; Fig 3).

Compared with pigeons of the same age injected with saline, pigeons treated with LPS showed significant shortening of the ileal villi, deeper crypts ($p < 0.05$, S2 Table and Fig 4), and a significantly decreased ratio of villus height/crypt depth (VH/CD) ($p < 0.01$, S2 Table and Fig 4).

Localization of TNF- α and IL-10 in the intestine

Positive immunohistochemical staining for TNF- α and IL-10 were predominantly detected in the cytoplasm, as indicated by brown staining. TNF- α and IL-10 were diffusely distributed in the villi, crypt, muscularis mucosa, muscular layer, and serosa and were predominant in the muscularis mucosa, muscular layer, and serosa. Significantly more positive areas of TNF- α and IL-10 staining were found in the intestine of LPS-treated Wahui pigeons than in that of

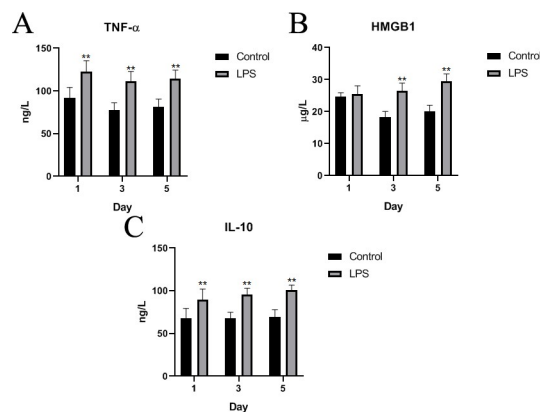


Fig 2. TNF- α , HMGB1, and IL-10 concentrations detected in the serum by ELISA on the first, third and fifth days. Data represent the mean \pm standard deviation ($n = 6$ in each group); * $p < 0.05$, ** $p < 0.01$.

<https://doi.org/10.1371/journal.pone.0251462.g002>

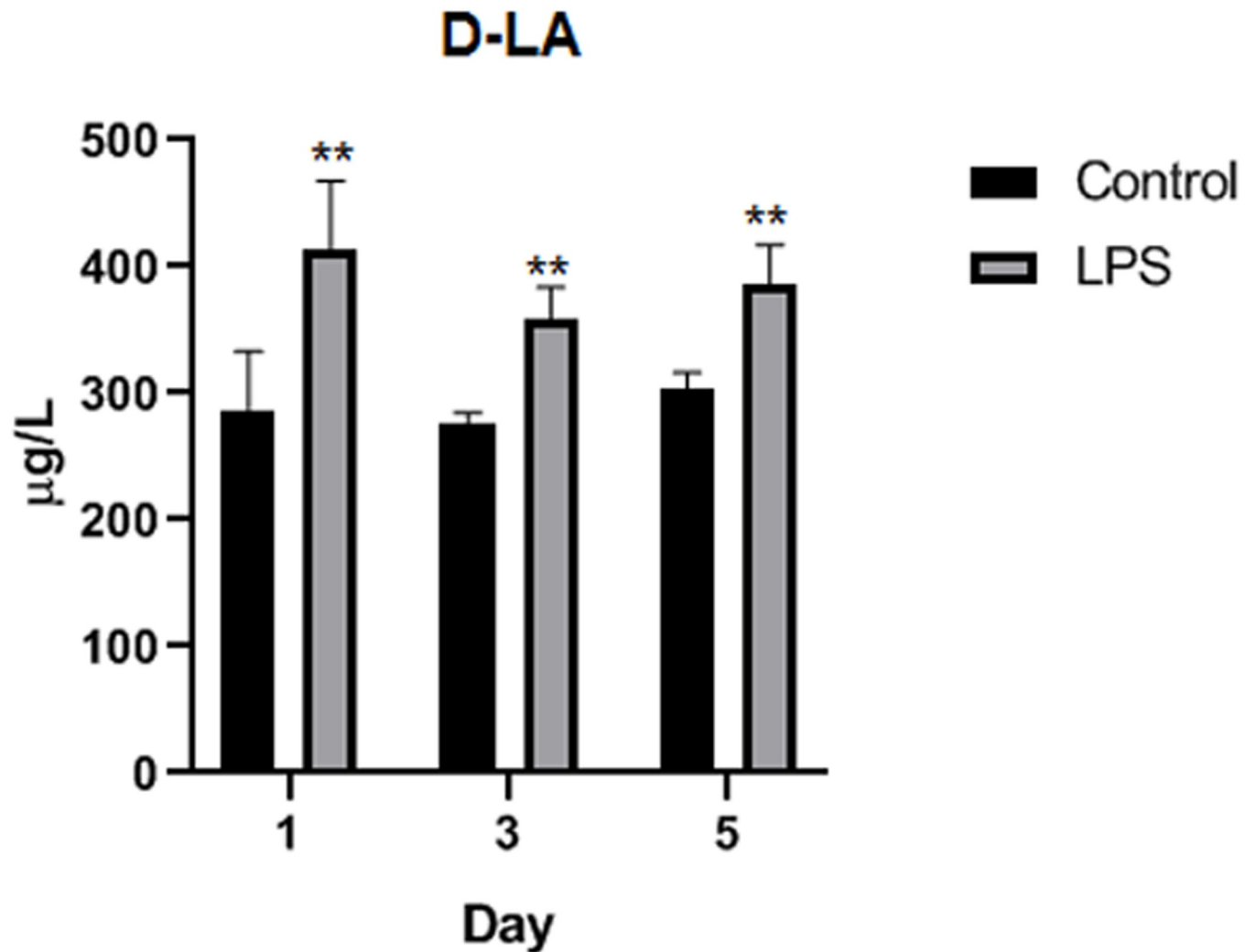


Fig 3. Detection of D-LA content in serum of Wahui pigeons. Data represent the mean \pm standard deviation (n = 6 in each group); *p < 0.05, **p < 0.01.

<https://doi.org/10.1371/journal.pone.0251462.g003>

saline-treated Wahui pigeons (Figs 5 and 6). The average optical density (AOD) was significantly different between the two groups on different days. The AOD of the TNF- α -positive cells was significantly higher in the LPS-treated Wahui pigeons than in the saline-treated pigeons on days 1, 3, and 5 (p < 0.01 for all three days; Fig 5D). The AOD of the IL-10-positive cells was higher in the LPS-treated Wahui pigeons than in the saline-treated pigeons on days 1, 3 and 5 (p < 0.01, p < 0.05, and p < 0.01, respectively; Fig 6D).

Occludin, Claudin3, and ZO-1 gene assays at intestinal tight junctions

As essential cell-cell junction for forming intestinal barrier, tight junction takes a role in structural strength and stability of intestine, the levels of gene expression, including Occludin, Claudin3, and ZO-1 related to tight junction, were detected. Compared to those in the control group, the expression levels of Occludin, Claudin3, and ZO-1 in the LPS group were significantly decreased on days 1, 3, and 5 (Fig 7). In addition, the expression levels of Occludin and Claudin3 in the LPS group showed a downward trend during the experiment (Fig 7A and 7B).

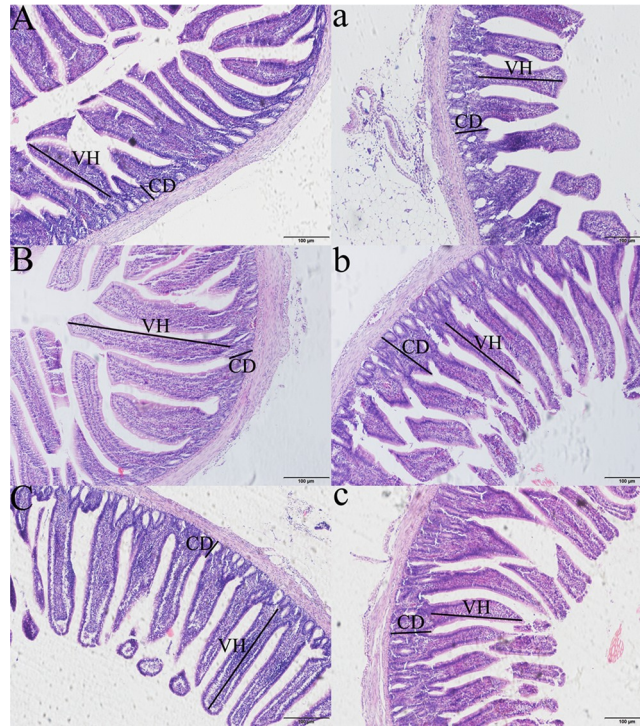


Fig 4. The intestinal microstructure of Wahui pigeons after LPS or saline treatment (100×). A, B, and C show the ileum of saline-treated Wahui pigeons on days 1, 3, and 5, respectively; a, b, and c show the ileum of LPS-treated Wahui pigeons on days 1, 3, and 5, respectively.

<https://doi.org/10.1371/journal.pone.0251462.g004>

Expression changes of key genes in multiple signaling pathways induced by LPS

In the autophagic signaling pathway, both factors showed similar results. *Atg5* expression in the LPS group was significantly higher than that in the control group on days 1, 3, and 5 ($p < 0.01$, $p < 0.05$, $p < 0.01$, respectively; Fig 8B), and Beclin1 expression was also significantly higher in the LPS group than in the control group on days 3 and 5 ($p < 0.01$ and $p < 0.05$, respectively), but the difference was not significant on day 1 (Fig 8A).

In the apoptotic signaling pathway, the expression level of Caspase-3 was significantly lower in the LPS group than in the control group on day 1 ($p < 0.05$); however, the expression levels of Caspase-3 and Bcl-2 were significantly increased on day 3 ($p < 0.01$ and $p < 0.01$, respectively) and were also elevated on day 5 ($p > 0.05$, Fig 8C and 8D).

In the inflammatory signaling pathway, TLR4 was expressed at a significantly lower level in the LPS group than in the control group ($p < 0.05$), while NF- κ B expression was significantly higher on day 1 ($p < 0.01$). The expression of TLR4, MyD88, and NF- κ B in the LPS-treated Wahui pigeons was significantly higher than that in the saline-treated pigeons on day 3 ($p < 0.01$, $p < 0.01$, and $p < 0.05$, respectively), but there were no significant differences between the two groups on day 5 ($p > 0.05$, Fig 8E–8G). On day 1, the TNF- α and IL-10 levels in the LPS group were significantly higher than those in the control group ($p < 0.05$ and $p < 0.01$, respectively). On day 3, the TNF- α and HMGB1 levels in the LPS group were significantly higher than those in the control group ($p < 0.01$ and $p < 0.05$, respectively). On day 5, the expression levels of HMGB1 and IL-10 in the LPS-treated pigeons were higher than those in the saline-treated pigeons ($p < 0.05$ and $p < 0.05$, respectively; Fig 8H–8J).

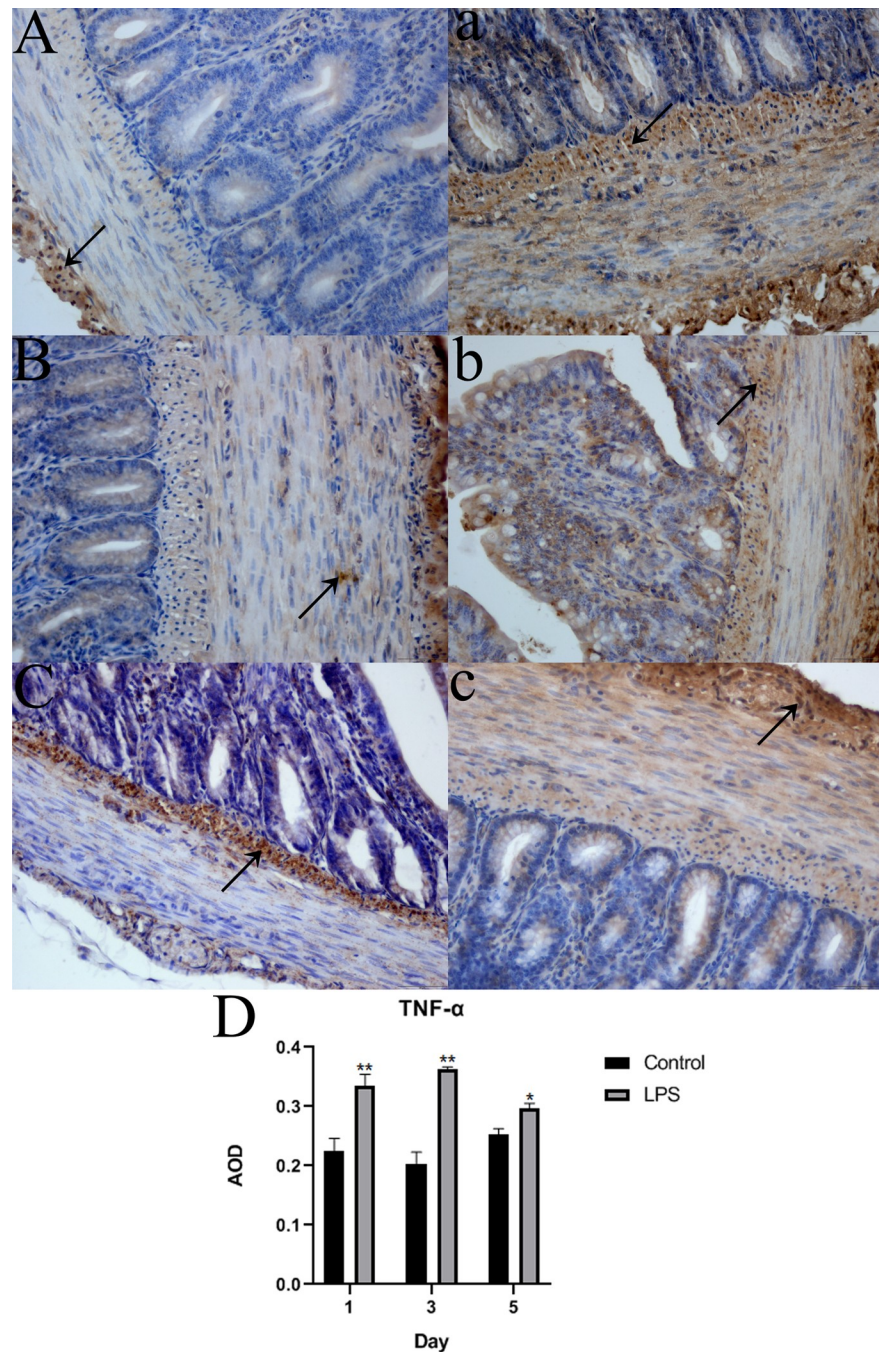


Fig 5. Detection of TNF- α in the ileum of LPS- and saline-treated Wahui pigeons. The black arrows indicate TNF- α -positive cells (400 \times). A, B, and C show the ileum of saline-treated Wahui pigeons on days 1, 3, and 5, respectively; a, b, and c show the ileum of LPS-treated Wahui pigeons on days 1, 3, 5, respectively. D: The average optical density (AOD) of TNF- α . Data represent the mean \pm standard deviation ($n = 6$ in each group), and six visual fields were evaluated in each section; * $p < 0.05$, ** $p < 0.01$.

<https://doi.org/10.1371/journal.pone.0251462.g005>

4. Discussion

The integrity of the intestine plays an essential role in nutrient absorption, gut homeostasis, and animal growth and health [18,19,28]. VH, CD, and the VH/CD ratio are common indices

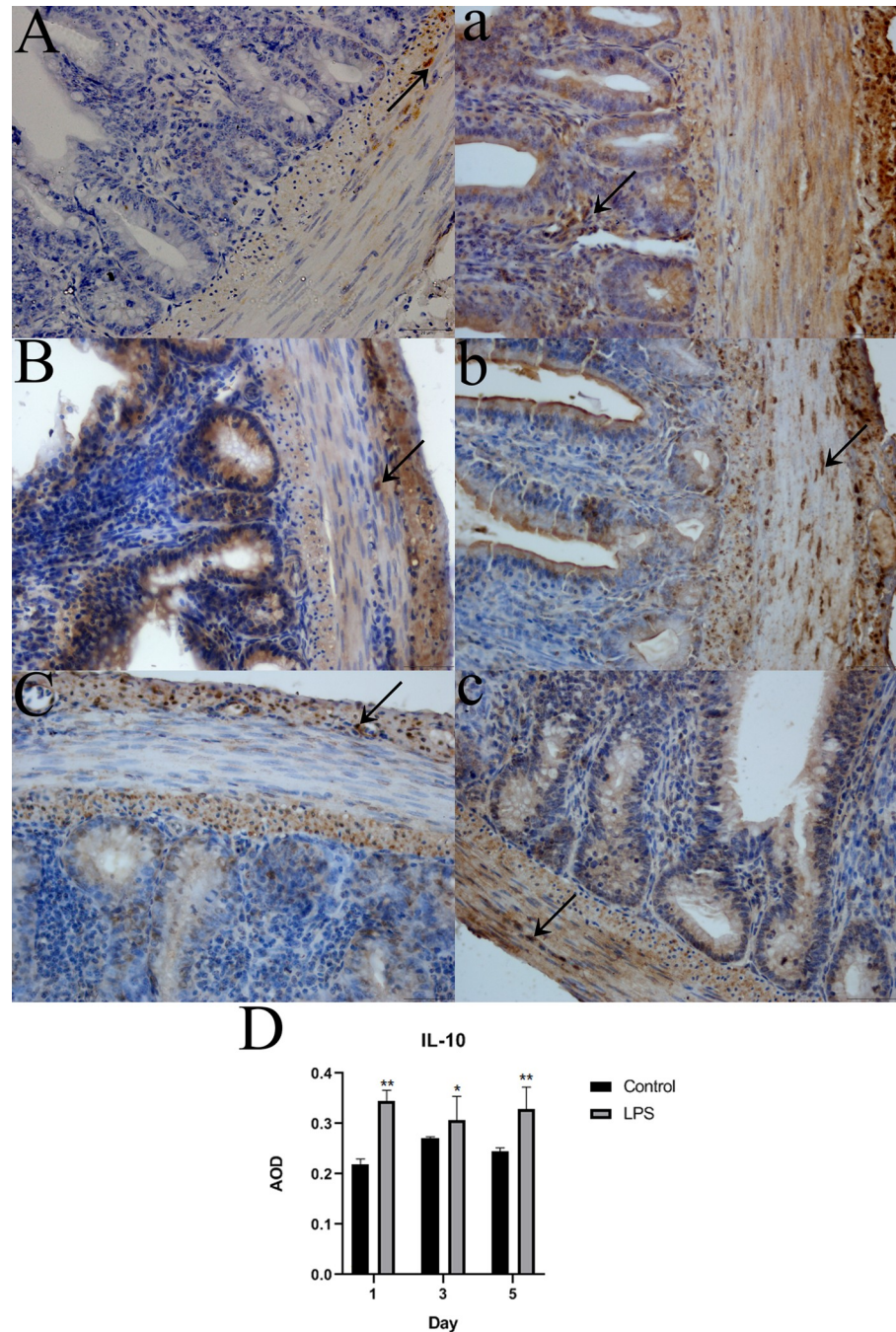


Fig 6. Detection of IL-10 in the ileum of LPS- and saline-treated Wahui pigeons. The black arrows indicate IL-10-positive cells (400 \times). A, B, and C show the ileum of saline-treated Wahui pigeons on days 1, 3, and 5, respectively; a, b, and c show the ileum of LPS-treated Wahui pigeons on days 1, 3, and 5, respectively. D: The average optical density (AOD) of IL-10. Data represent the mean \pm standard deviation ($n = 6$ in each group), and six visual fields were evaluated in each section; * $p < 0.05$, ** $p < 0.01$.

<https://doi.org/10.1371/journal.pone.0251462.g006>

for evaluating intestinal morphology [18]. The reason these indices are used is related to the fact that an increased VH and elevated VH/CD are directly correlated with increased epithelial turnover [30], and longer villi are linked with the activation of cell mitosis, while shortening of

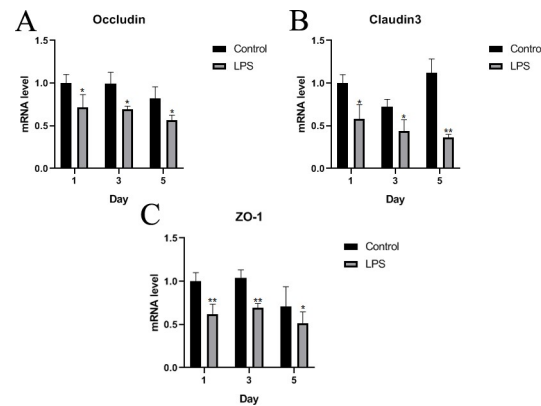


Fig 7. Evaluation of the intestinal tight junctions of Wahui pigeons treated with LPS or saline. The mRNA expression of Occludin, Claudin3, and ZO-1 in the ileum was detected by RT-qPCR on the first, third, and fifth days after LPS or saline treatment, and *GAPDH* was used as a reference gene. Data represent the mean \pm standard deviation ($n = 6$ in each group); For Wahui pigeons of the same age, * $p < 0.05$ and ** $p < 0.01$.

<https://doi.org/10.1371/journal.pone.0251462.g007>

villi and deeper crypts lead to poor nutrient absorption [31], increased secretion in the gastrointestinal tract, and reduced performance [32]. A change in the integrity of the intestinal barrier induced by LPS can be detected by monitoring morphological changes in the intact intestinal villi and detecting chemical markers. Morphological changes in the intact intestinal villi are an indication of intestinal barrier injury, including LPS-induced injury [33,34]. D-LA is produced by intestinal microorganisms in vivo. When the intestinal mucosa is damaged and its permeability increases, D-LA will enter the blood, resulting in an increase in the serum D-LA level. The content of serum D-LA therefore reflects the health of the intestinal tract [35]. The present study demonstrated acute intestinal damage, with broken intestinal villi, a shortened VH, and an increased CD in the ileum, accompanied by higher D-LA levels in the serum.

It has been indicated that tight junctions between intestinal epithelial cells play an irreplaceable role in the function of the intestinal barrier [36]. Tight junctions act as receptors or targets of bacterial virulence factors during the infection of a range of viral and bacterial pathogens. Disruption of tight junctions leads to increased epithelial permeability and facilitates the translocation of pathogens into the body and colonization, usually resulting in diarrhea [37]. Increased expression of tight junction proteins enhances the function of the intestinal mucosal barrier. A series of proteins, including Claudins, Occludins, and ZOs, contribute to the formation of tight junctions. Numerous studies have reported that Occludin, Claudin3, and ZO-1 are key components of tight junction complexes and play important roles in intestinal permeability [38–40]. In the current study, the mRNA expression levels of Occludin, Claudin3, and ZO-1 were significantly decreased in the ileum of Wahui pigeons after LPS administration, suggesting that the intestinal barrier was damaged during injury.

Dysfunction of the intestinal barrier can increase intestinal mucosal permeability, induce the translocation of enteric pathogenic organisms, and in turn exacerbate the loss of intestinal barrier integrity. This can lead to systemic infection, multiorgan failure, and septic shock, which is a common pathological progression in many intestinal diseases [41]. A previous report showed that LPS exposure could lead to oxidative stress in the intestine [42]. LPS administration induces systemic and intestinal inflammation, accompanied by intestinal oxidative stress and increased intestinal permeability [4]. ROS are not only byproducts of inflammatory processes but also capable of causing damage to epithelial cell integrity and are closely linked to apoptosis in a variety of cell types [20]. Evidence from intestinal epithelial cells shows that elevated oxidative stress can inhibit cell proliferation and induce apoptosis [20,43]. In

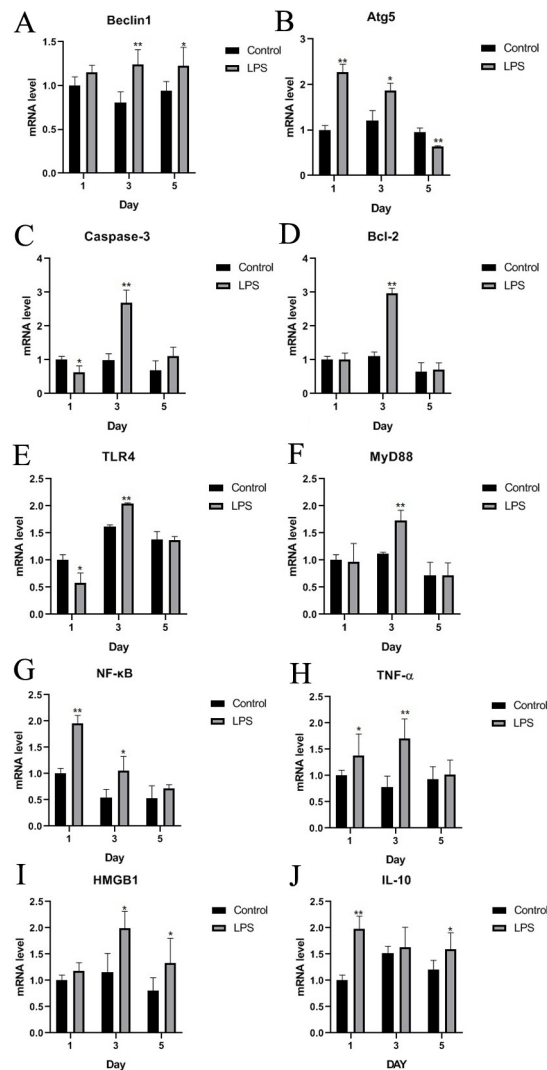


Fig 8. Levels of indicators of various signaling pathways in Wahui pigeons treated with LPS or saline. The mRNA expression levels of Beclin1, Atg5, Caspase-3, Bcl-2, TLR4, MyD88, NF- κ B, TNF- α , HMGB1, and IL-10 were detected by RT-qPCR on the first, third, and fifth days after LPS or saline treatment, and *GAPDH* was used as a reference gene. Data represent the mean \pm standard deviation ($n = 6$ in each group); For Wahui pigeons of the same age, * $p < 0.05$ and ** $p < 0.01$.

<https://doi.org/10.1371/journal.pone.0251462.g008>

animals, there are many antioxidant enzymes and nonenzymatic antioxidants that protect the organism from oxidative damage [44]. MDA, as a product of lipid peroxidation, is acknowledged to be an index of cellular damage and excessive oxidative stress [45]. SOD converts superoxide (O_2^-) into H_2O_2 , which is dissociated into H_2O by CAT [46]. SOD levels indirectly reflect the capacity of organisms to neutralize ROS, and MDA content reflects the severity of the body's exposure to free radicals [47]. In the current study, the levels of CAT and GSH were significantly decreased, but that of MDA was increased, indicating that oxidative stress occurred in the pigeons as a result of LPS treatment.

Oxidative stress and redox signaling can induce the release of proinflammatory factors, and the course of "ROS-induced inflammation" has been considered a contributor in the progression of most chronic diseases [48]. When foreign microorganisms invade, the innate immune system is activated to regulate antigen-presenting cells and initiate acquired

immunity in the body. As an innate immune pattern recognition receptor, TLR4 can specifically recognize LPS from the outer membrane of gram-negative bacteria and forms the first line of defense called innate immunity. LPS binds to TLR4/MD2 to form a complex that selectively activates the MyD88-dependent pathway, resulting in the activation of the transcription factor NF- κ B [49]. NF- κ B plays important roles in the regulation of cytokines, adhesion molecules, inflammation, and oxidative stress and is also an important regulator of the intracellular inflammatory cascade. Numerous proinflammatory signals, including TNF- α and IFN- γ , promptly activate NF- κ B to control target genes. Activated NF- κ B enters the nucleus and stimulates the expression of a variety of genes that participate in immunoregulation and inflammatory reactions [50]. TNF- α is not only a factor related to the systemic inflammatory response but also the most important cytokine that causes an acute inflammatory response [51]. TNF- α is secreted mainly by macrophages, which activates macrophages to release a large number of proinflammatory factors, such as IL-1 β , IL-6, and IFN- γ , through feedback regulation. This feedback plays a central role in the regulation of inflammation. TNF- α can also act as an endogenous pyrogen, causing fever and apoptosis [52,53]. HMGB1 is a fatal inflammatory factor caused by sepsis. Its release occurs later than that of inflammatory cytokines (such as IL-1 β , IL-6, and TNF- α), and it is called a late risk signal factor [54]. HMGB1 activates *Aspergillus fumigatus* in alveolar macrophages in chronic obstructive pulmonary disease through the MyD88/NF- κ B and syk/PI3K signal transduction pathways, leading to inflammation [55]. It has been reported that glycyrrhizic acid, an inhibitor of HMGB1, can mediate renal injury and inflammation in diabetic rats by regulating the activation of the RAGE/TLR4-related ERK and p38MAPK/NF- κ B signaling pathways [56]. In addition, HMGB1 is overexpressed in thyroid cancer patient samples and cell lines and acts as a positive regulator of autophagy [57]. The stress in piglets responding to LPS challenge results in increased levels of proinflammatory cytokines [58,59]. In the present study, the mRNA expression levels of TNF- α , HMGB1, and IL-10 were increased in the ileum; the contents of TNF- α , HMGB1, and IL-10 were relatively high in the serum; and the protein levels of TNF- α and IL-10 were relatively high in the ileum. These findings suggest that LPS causes an inflammatory response could regulate by the TLR4/MyD88/NF- κ B signaling pathway in Wuhui pigeons.

It has been reported that a variety of Toll-like receptor ligands, such as double-stranded RNA and LPS, can lead to apoptosis [60–62]. As an important transcription factor, NF- κ B not only controls inflammation but also acts in apoptosis [63]. NF- κ B induces a variety of antiapoptotic factors, including inhibitors of caspase activation and activity, antiapoptotic Bcl-2 family members, and inhibitors of Jnk activation, which can prevent TNF- α -induced apoptosis [64]. Caspase-3 is another apoptosis-induced protein. Caspases generally play a central role in apoptosis induction [65]. Autophagy can be induced by a variety of stimuli and upstream signaling changes, including activation of the TLR4 signaling pathway. The pathogen-associated molecular molecule LPS activates the TLR4 signaling pathway and increases the level of autophagy in macrophages [66]. Another study demonstrated that LPS-induced autophagy is a TRIF-dependent and MyD88-independent signaling pathway [66]. Autophagy activated by TLR4 is regulated by the interaction of MyD88 and TRIF with Beclin-1 [67]. Binding of TLR4 with ligands induces the molecular interaction of MyD88, TRIF, and Beclin-1 but reduces the binding between Bcl-2 and Beclin-1, relieving the inhibition of Beclin-1 by Bcl-2 and promoting the occurrence of autophagy [67]. An NF- κ B inhibitor, SN50, was found to inhibit NF- κ B nuclear translocation and activate autophagy [68]. The key genes of autophagy and apoptosis pathway were almost continuously expressed at a high level after LPS challenge here, the intestinal injury probably took place along with autophagy and apoptosis of ileal cells.

5. Conclusion

In summary, continuous LPS challenge can induce oxidative stress, which promotes the release of inflammatory mediators, activates local and/or systemic inflammatory responses, causes apoptosis and autophagy, and reduces the expression of tight junction proteins, resulting in intestinal barrier dysfunction, thus reducing intestinal immunity and eventually leading to intestinal injury. This provides novel evidence for the pathological mechanism of intestine induced by *Salmonella* LPS in pigeon.

Supporting information

S1 Table. The primer sequences applied in real-time PCR.

(DOCX)

S2 Table. Morphological changes induced by LPS in the ileum of Wahui pigeons.

(DOCX)

Author Contributions

Conceptualization: Fei Wang, Jin Liu, Yong Li.

Data curation: Fei Wang, Jin Liu.

Formal analysis: Fei Wang, Xu Yuan.

Investigation: Xiaofen Hu, Youbao Zhong, Feng Wen, Xiaoen Tang, Zuohong Zhou.

Methodology: Fei Wang, Shanshan Yang, Shengwei Zhong.

Writing – original draft: Fei Wang, Jin Liu.

Writing – review & editing: Fei Wang, Jin Liu, Yong Li.

References

1. Valceschini EY. Poultry meat trends and consumer attitudes. Proc EPC 2006-12th European Poultry Conference, Verona, Italy. 2006; 10–14 September.
2. Jones JW, Shaffer SA, Ernst RK, Goodlett DR, Turecek F. Determination of pyrophosphorylated forms of lipid A in Gram-negative bacteria using a multivariate mass spectrometric approach. Proc Natl Acad Sci USA. 2008; 105(35):12742–12747. <https://doi.org/10.1073/pnas.0800445105> PMID: 18753624
3. Rosas-Ballina M, Ochani M, Parrish WR, Ochani K, Harris YT, Huston JM, et al. Splenic nerve is required for cholinergic antiinflammatory pathway control of TNF in endotoxemia. Proceedings of the National Academy of Sciences. 2008; 105(31):11008–11013. <https://doi.org/10.1073/pnas.0803237105> PMID: 18669662
4. Gil-Cardoso K, Comitato R, Gines I, Ardevol A, Pinent M, Virgili F, et al. Protective effect of proanthocyanidins in a rat model of mild intestinal inflammation and impaired intestinal permeability induced by LPS. Mol Nutr Food Res. 2019; 63(8):e1800720. <https://doi.org/10.1002/mnfr.201800720> PMID: 30656830
5. Pillich H, Loose M, Zimmer KP, Chakraborty T. Diverse roles of endoplasmic reticulum stress sensors in bacterial infection. Molecular and Cellular Pediatrics. 2016; 3(1):9. <https://doi.org/10.1186/s40348-016-0037-7> PMID: 26883353
6. Goebel A, Kavanagh E, Lyons A, Saporoschetz IB, Soberg C, Lederer JA, et al. Injury induces deficient interleukin-12 production, but interleukin-12 therapy after injury restores resistance to infection. Annals of Surgery. 2000; 231(2):253. <https://doi.org/10.1097/0000658-200002000-00015> PMID: 10674618
7. Chen L, Li S, Zheng J, Li WT, Jiang XM, Zhao XL, et al. Effects of dietary *Clostridium butyricum* supplementation on growth performance, intestinal development, and immune response of weaned piglets challenged with lipopolysaccharide. J Anim Sci Biotechnol. 2018; 9:62. <https://doi.org/10.1186/s40104-018-0275-8> PMID: 30159141

8. Lee SI, Kang KS. N-acetylcysteine modulates lipopolysaccharide-induced intestinal dysfunction. *Sci Rep*. 2019; 9(1):1004. <https://doi.org/10.1038/s41598-018-37296-x> PMID: 30700808
9. Mittal M, Siddiqui MR, Tran K, Reddy SP, Malik AB. Reactive oxygen species in inflammation and tissue injury. *Antioxid Redox Signal*. 2014; 20(7):1126–1167. <https://doi.org/10.1089/ars.2012.5149> PMID: 23991888
10. Wu WC, Wang YZ, Shan TZ, Wang SS, Liu Q. Metformin protects against LPS-induced intestinal barrier dysfunction by activating AMPK pathway. *Mol Pharm*. 2018; 15(8):3272–3284. <https://doi.org/10.1021/acs.molpharmaceut.8b00332> PMID: 29969038
11. Yang F, Liao JZ, Pei RN, Yu WL, Han QY, Li Y, et al. Autophagy attenuates copper-induced mitochondrial dysfunction by regulating oxidative stress in chicken hepatocytes. *Chemosphere*. 2018; 204:36–43. <https://doi.org/10.1016/j.chemosphere.2018.03.192> PMID: 29649662
12. Yang F, Pei RN, Zhang ZW, Liao JZ, Yu WL, Qiao Na, et al. Copper induces oxidative stress and apoptosis through mitochondria-mediated pathway in chicken hepatocytes. *Toxicol in Vitro*. 2019; 54:310–316. <https://doi.org/10.1016/j.tiv.2018.10.017> PMID: 30389602
13. Song ZH, Tong G, Xiao K, Jiao LF, Ke YL, Hu CH. L-Cysteine protects intestinal integrity, attenuates intestinal inflammation and oxidant stress, and modulates NF- κ B and Nrf2 pathways in weaned piglets after LPS challenge. *Innate Immunity*. 2016; 22(3):152–161. <https://doi.org/10.1177/1753425916632303> PMID: 26921254
14. Zhang H, Sun SC. NF- κ B in inflammation and renal diseases. *Cell Biosci*. 2015; 5:63. <https://doi.org/10.1186/s13578-015-0056-4> PMID: 26579219
15. Mann M, Mehta A, Zhao JL, Lee K, Marinov GK, Garcia-Flores Y, et al. An NF- κ B-microRNA regulatory network tunes macrophage inflammatory responses. *Nat Commun*. 2017; 8(1):851. <https://doi.org/10.1038/s41467-017-00972-z> PMID: 29021573
16. Newton K, Dixit VM. Signaling in innate immunity and inflammation. *Cold Spring Harb Perspect Biol*. 2012; 4(3):a006049. <https://doi.org/10.1101/cshperspect.a006049> PMID: 22296764
17. Sukhotnik I, Haj B, Pollak Y, Dorfman T, Bejar J, Matter I. Effect of bowel resection on TLR signaling during intestinal adaptation in a rat model. *Surg Endosc*. 2016; 30(10):4416–4424. <https://doi.org/10.1007/s00464-016-4760-x> PMID: 26895894
18. Wijtten PJA, van der Meulen J, Versteegen MWA. Intestinal barrier function and absorption in pigs after weaning: a review. *Br J Nutr*. 2011; 105(7):967–981. <https://doi.org/10.1017/S0007114510005660> PMID: 21303573
19. Blikslager AT, Moeser AJ, Gookin JL, Jones SL, Odle J. Restoration of barrier function in injured intestinal mucosa. *Physiol Rev*. 2007; 87(2):545–564. <https://doi.org/10.1152/physrev.00012.2006> PMID: 17429041
20. Oz HS, Chen TS, Nagasawa H. Comparative efficacies of 2 cysteine prodrugs and a glutathione delivery agent in a colitis model. *Transl Res*. 2007; 150(2):122–129. <https://doi.org/10.1016/j.trsl.2006.12.010> PMID: 17656332
21. Oz HS, Chen TS, McClain CJ, de Villiers WJS. Antioxidants as novel therapy in a murine model of colitis. *J Nutr Biochem*. 2005; 16(5):297–304. <https://doi.org/10.1016/j.jnutbio.2004.09.007> PMID: 15866230
22. Liu YL, Chen F, Odle J, Lin X, Jacobi SK, Zhu HL, et al. Fish oil enhances intestinal integrity and inhibits TLR4 and NOD2 signaling pathways in weaned pigs after LPS challenge. *J Nutr*. 2012; 142(11):2017–2024. <https://doi.org/10.3945/jn.112.164947> PMID: 23014495
23. Guo SH, Al-Sadi R, Said HM, Ma TY. Lipopolysaccharide causes an increase in intestinal tight junction permeability in vitro and in vivo by inducing enterocyte membrane expression and localization of TLR-4 and CD14. *Am J Pathol*. 2013; 182(2):375–387. <https://doi.org/10.1016/j.ajpath.2012.10.014> PMID: 23201091
24. Nochi T, Jansen CA, Toyomizu M, van Eden W. The well-developed mucosal immune systems of birds and mammals allow for similar approaches of mucosal vaccination in both types of animals. *Front Nutr*. 2018; 5:60. <https://doi.org/10.3389/fnut.2018.00060> PMID: 30050906
25. Zhou L, Huang S, Luo X, Su Y. Advances in intestinal mucosal immunity provides an opportunity for traditional Chinese medicine immunity research. *Chin J Immunol*. 2019; 35:2945–2952. (in Chinese)
26. Zhong YB, Zhang XL, Lv MY, Hu XF, Li Y. Detection of IL-1 β , IL-6 and TNF- α in Sprague-Dawley rats' atrophic thymus induced by lipopolysaccharide. *Pol J Vet Sci*. 2018; 21(3):589–597. <https://doi.org/10.24425/124294> PMID: 30468342
27. Zhong YB, Hu XF, Guo H, Li Y. Skp2 expression exhibits a negative correlation with P27Kip1 in lungs of SD rat stress model induced by lipopolysaccharide. *Indian J Anim Res*. 2017; 51(6):1019–1026.
28. Circu ML, Aw TY. Intestinal redox biology and oxidative stress. *Semin Cell Dev Biol*. 2012; 23(7):729–737. <https://doi.org/10.1016/j.semcdb.2012.03.014> PMID: 22484611

29. Ji JJ, Gu ZT, Li H, Su L, Liu ZF. Cryptdin-2 predicts intestinal injury during heatstroke in mice. *Int J Mol Med*. 2018; 41(1):137–146. <https://doi.org/10.3892/ijmm.2017.3229> PMID: 29115396
30. Ichikawa H, Kuroiwa T, Inagaki A, Shineha R, Nishihira T, Satomi S, et al. Probiotic bacteria stimulate gut epithelial cell proliferation in rat. *Dig Dis Sci*. 1999; 44(10):2119–2123. <https://doi.org/10.1023/a:1026647024077> PMID: 10548366
31. Nyachoti CM, Omogbenigun FO, Rademacher M, Blank G. Performance responses and indicators of gastrointestinal health in early-weaned pigs fed low-protein amino acid-supplemented diets. *J Anim Sci*. 2006; 84(1):125–134. <https://doi.org/10.2527/2006.841125x> PMID: 16361499
32. Hossain MM, Begum M, Kim IH. Effect of *Bacillus subtilis*, *Clostridium butyricum* and *Lactobacillus acidophilus* endospores on growth performance, nutrient digestibility, meat quality, relative organ weight, microbial shedding and excreta noxious gas emission in broilers. *Vet Med-Czech*. 2015; 60(2):77–86.
33. Effenberger-Neidnicht K, Jagers J, Verhaegh R, de Groot H. Glycine selectively reduces intestinal injury during endotoxemia. *J Surg Res*. 2014; 192(2):592–598. <https://doi.org/10.1016/j.jss.2014.06.016> PMID: 25012270
34. Song WB, Wang YY, Meng FS, Zhang QH, Zeng JY, Xiao LP, et al. Curcumin protects intestinal mucosal barrier function of rat enteritis via activation of MKP-1 and attenuation of p38 and NF- κ B activation. *PLoS One*. 2010; 5(9):e12969. <https://doi.org/10.1371/journal.pone.0012969> PMID: 20885979
35. Li QZ, Li ZL, Li JY, Lu LR, Li JY. Evaluation of intestinal barrier function after abdominal surgery by plasma D-lactic acid level. *Med J Chin PLA*. 2005; 30:255–257. (in Chinese)
36. Hou YQ, Wang L, Zhang W, Yang ZG, Ding BY, Zhu HL, et al. Protective effects of N-acetylcysteine on intestinal functions of piglets challenged with lipopolysaccharide. *Amino Acids*. 2012; 43(3):1233–1242. <https://doi.org/10.1007/s00726-011-1191-9> PMID: 22180025
37. Konig J, Wells J, Cani PD, Garcia-Rodenas CL, MacDonald T, Mercenier A, et al. Human intestinal barrier function in health and disease. *Clin Transl Gastroen*. 2016; 7(10):e196. <https://doi.org/10.1038/ctg.2016.54> PMID: 27763627
38. Van Itallie CM, Fanning AS, Holmes J, Anderson JM. Occludin is required for cytokine-induced regulation of tight junction barriers. *J Cell Sci*. 2010; 123(Pt 16):2844–2852. <https://doi.org/10.1242/jcs.065581> PMID: 20663912
39. Vergauwen H, Degroote J, Prims S, Prims S, Wang W, Fransens E, et al. Artificial rearing influences the morphology, permeability and redox state of the gastrointestinal tract of low and normal birth weight piglets. *J Anim Sci Biotechnol*. 2017; 8:30. <https://doi.org/10.1186/s40104-017-0159-3> PMID: 28405313
40. Tsukita S, Furuse M, Itoh M. Multifunctional strands in tight junctions. *Nat Rev Mol Cell Biol*. 2001; 2(4):285–293. <https://doi.org/10.1038/35067088> PMID: 11283726
41. Lamprecht G, Heininger A. Current aspects of sepsis caused by bacterial translocation. *Zentralbl Chir*. 2012; 137(3):274–278. <https://doi.org/10.1055/s-0031-1284043> PMID: 22711326
42. Wu GJ, Zhou WH, Zhao JF, Pan XH, Sun YJ, Xu H, et al. Matrine alleviates inflammation and oxidative stress via CCR7 signal intestinal. *Oncotarget*. 2017; 8(7):11621–11628. <https://doi.org/10.18632/oncotarget.14598> PMID: 28086227
43. Jonas CR, Ziegler TR, Gu LH, Jones DP. Extracellular thiol/disulfide redox state affects proliferation rate in a human colon carcinoma (Caco2) cell line. *Free Radic Bio Med*. 2002; 33(11):1499–1506.
44. Yin J, Liu MF, Ren WK, Duan JL, Yang G, Zhao YR, et al. Effects of dietary supplementation with glutamate and aspartate on diquat-induced oxidative stress in piglets. *PLoS One*. 2015; 10(4):e122893. <https://doi.org/10.1371/journal.pone.0122893> PMID: 25875335
45. Mao GH, Li Q, Deng CM, Wang YQ, Ding YY, Zhang WJ, et al. The synergism and attenuation effect of Selenium (Se)-enriched *Grifola frondosa* (Se)-polysaccharide on 5-Fluorouracil (5-Fu) in Hep3-bearing mice. *Int J Biol Macromol*. 2018; 107(Pt B):2211–2216. <https://doi.org/10.1016/j.jbiomac.2017.10.084> PMID: 29042284
46. Zhang C, Ge J, Lv MW, Zhang Q, Talukder M, Li JL. Selenium prevent cadmium-induced hepatotoxicity through modulation of endoplasmic reticulum-resident selenoproteins and attenuation of endoplasmic reticulum stress. *Environ Pollut*. 2020; 260:113873. <https://doi.org/10.1016/j.envpol.2019.113873> PMID: 32369892
47. Zhou XR, Zhao L, Luo J, Tang HQ, Xu M, Wang YY, et al. The toxic effects and mechanisms of nano-Cu on the spleen of rats. *Int J Mol Sci*. 2019; 20(6):1469. <https://doi.org/10.3390/ijms20061469> PMID: 30909528
48. Sturza A, Popoiu CM, Ionica M, Duicu OM, Olariu S, Danina MM, et al. Monoamine oxidase-related vascular oxidative stress in diseases associated with inflammatory burden. *Oxid Med Cell Longev*. 2019; 2019(1):1–8. <https://doi.org/10.1155/2019/8954201> PMID: 31178977
49. Keestra AM, van Putten JPM. Unique properties of the chicken TLR4/MD-2 complex: selective lipopolysaccharide activation of the MyD88-dependent pathway. *Journal of Immunology*. 2008; 181(6):4354–4362.

50. Zhao HJ, Wang Y, Shao YZ, Liu JJ, Wang SR, Xing MW. Oxidative stress-induced skeletal muscle injury involves in NF-kappaB/p53-activated immunosuppression and apoptosis response in copper (II) or/and arsenite-exposed chicken. *Chemosphere*. 2018; 210:76–84. <https://doi.org/10.1016/j.chemosphere.2018.06.165> PMID: 29986226
51. Gao BH. The role of TNF in inflammation. *Chin J Postgra Med*. 1999; 22:55–56. (in Chinese)
52. Cnop M, Welsh N, Jonas JC, Jorns A, Lenzen S, Eizirik DL. Mechanisms of pancreatic beta-cell death in type 1 and type 2 diabetes: many differences, few similarities. *Diabetes*. 2005; 54(Suppl 2):S97–S107. https://doi.org/10.2337/diabetes.54.suppl_2.s97 PMID: 16306347
53. Muppidi JR, Tschopp J, Siegel RM. Life and death decisions: secondary complexes and lipid rafts in TNF receptor family signal transduction. *Immunity*. 2004; 21(4):461–465. <https://doi.org/10.1016/j.immuni.2004.10.001> PMID: 15485624
54. Splichalova A, Splichal I. Local and systemic occurrences of HMGB1 in gnotobiotic piglets infected with *E. coli* O55 are related to bacterial translocation and inflammatory cytokines. *Cytokine*. 2012; 60(3):597–600. <https://doi.org/10.1016/j.cyto.2012.07.026> PMID: 22902066
55. Zhang PP, Xin XF, Fang LP, Jiang H, Xu XY, Su X, et al. HMGB1 mediates *Aspergillus fumigatus*-induced inflammatory response in alveolar macrophages of COPD mice via activating MyD88/NF- κ B and syk/PI3K signalings. *Int Immunopharmacol*. 2017; 53:125–132. <https://doi.org/10.1016/j.intimp.2017.10.007> PMID: 29078091
56. Zhang H, Zhang R, Chen J, Shi M, Li W, Zhang XC. High mobility group box I inhibitor Glycyrrhizic acid attenuates kidney injury in streptozotocin-induced diabetic rats. *Kidney Blood Press Res*. 2017; 42(5):894–904. <https://doi.org/10.1159/000485045> PMID: 29241180
57. Chai WW, Ye FH, Zeng L, Li YL, Yang LC. HMGB1-mediated autophagy regulates sodium/iodide symporter protein degradation in thyroid cancer cells. *J Exp Clin Cancer Res*. 2019; 38(1):325. <https://doi.org/10.1186/s13046-019-1328-3> PMID: 31331356
58. Qiu YS, Zhang JW, Liu Y, Ma HW, Cao FY, Xu J, et al. The combination effects of acetaminophen and N-acetylcysteine on cytokines production and NF-kappaB activation of lipopolysaccharide-challenged piglet mononuclear phagocytes in vitro and in vivo. *Vet Immunol Immunopathol*. 2013; 152(3–4):381–388. <https://doi.org/10.1016/j.vetimm.2013.01.013> PMID: 23434081
59. Wang QJ, Hou YQ, Yi D, Wang L, Ding BY, Chen X, et al. Protective effects of N-acetylcysteine on acetic acid-induced colitis in a porcine model. *BMC Gastroenterol*. 2013; 13:133. <https://doi.org/10.1186/1471-230X-13-133> PMID: 24001404
60. Aliprantis AO, Yang RB, Weiss DS, Godowski P, Zychlinsky A. The apoptotic signaling pathway activated by Toll-like receptor-2. *EMBO J*. 2000; 19(13):3325–3336. <https://doi.org/10.1093/emboj/19.13.3325> PMID: 10880445
61. Bannerman DD, Tupper JC, Kelly JD, Winn RK, Harlan JM. The Fas-associated death domain protein suppresses activation of NF-kappa B by LPS and IL-1 beta. *J Clin Invest*. 2002; 109(3):419–425. <https://doi.org/10.1172/JCI14774> PMID: 11828002
62. Hsu LC, Park JM, Zhong K, Luo JL, Maeda S, Kaufman RJ, et al. The protein kinase PKR is required for macrophage apoptosis after activation of Toll-like receptor 4. *Nature*. 2004; 428(6980):341–345. <https://doi.org/10.1038/nature02405> PMID: 15029200
63. He LX, Zhang ZF, Zhao J, Li L, Xu T, Sun B, et al. Ginseng oligopeptides protect against irradiation-induced immune dysfunction and intestinal injury. *Sci Rep*. 2018; 8(1):13916. <https://doi.org/10.1038/s41598-018-32188-6> PMID: 30224720
64. Karin M, Lin A. NF-kappaB at the crossroads of life and death. *Nat Immunol*. 2002; 3(3):221–227. <https://doi.org/10.1038/ni0302-221> PMID: 11875461
65. Modjtahedi N, Giordanetto F, Madeo F, Kroemer G. Apoptosis-inducing factor: vital and lethal. *Trends Cell Biol*. 2006; 16(5):264–272. <https://doi.org/10.1016/j.tcb.2006.03.008> PMID: 16621561
66. Xu Y, Jagannath C, Liu XD, Sharafkhaneh A, Kolodziejaska KE, Eissa NT. Toll-like receptor 4 is a sensor for autophagy associated with innate immunity. *Immunity*. 2007; 27(1):135–144. <https://doi.org/10.1016/j.immuni.2007.05.022> PMID: 17658277
67. Shi CS, Kehrl JH. MyD88 and TRIF target Beclin 1 to trigger autophagy in macrophages. *J Biol Chem*. 2008; 283(48):33175–33182. <https://doi.org/10.1074/jbc.M804478200> PMID: 18772134
68. Zhu BS, Xing CG, Lin F, Fan XQ, Zhao K, Qin ZH. Blocking NF- κ B nuclear translocation leads to p53-related autophagy activation and cell apoptosis. *World J Gastroenterol*. 2011; 17(4):478–487. <https://doi.org/10.3748/wjg.v17.i4.478> PMID: 21274377